IEEE Open Journal of Nanotechnology

Received 3 November 2022; revised 10 November 2022; accepted 15 November 2022. Date of publication 21 November 2022; date of current version 3 February 2023. The review of this article was arranged by Associate Editor Xinge Yu.

Digital Object Identifier 10.1109/OJNANO.2022.3223712

Droplet-Dispensed Graphene Oxide as Capacitive Sensing Elements for Flexible Pressure-Pulse Sensing Array

KA WAI KONG[1,2], KEER WANG[1,3], ALICE YEUK LAN LEUNG[4], HONGYU ZHANG[1], JIAO SUO[1], MENG CHEN[1], GUANGLIE ZHANG[1,2], FEI FEI[3], JIANGANG SHEN[4], AND WEN JUNG LI[1,2] (Fellow, IEEE)

[1]Department of Mechanical Engineering, City University of Hong Kong, Hong Kong, SAR 999077, China
[2]CAS-CityU Joint Lab for Robotics Research, City University of Hong Kong Shenzhen Research Institute, Shenzhen 518057, China
[3]College of Automation Engineering, Nanjing University of Aeronautics and Astronautics, Nanjing 211100, China
[4]School of Chinese Medicine, The University of Hong Kong, Hong Kong, SAR 999077, China

CORRESPONDING AUTHORS: FEI FEI; JIANGANG SHEN; WEN JUNG LI (e-mail: alex.ffei@foxmail.com; shenjg@hku.h; wenjli@cityu.edu.hk).

This work was supported in part by the Hong Kong Research Grants Council through GRF Project under Grants 11204918 and 11216120 and in part by the Hong Kong Health Bureau through HMRF Project under Grant 17181811. *(Ka Wai Kong and Keer Wang contributed equally to this work.)*

ABSTRACT We report a novel flexible capacitive pressure-pulse sensor array developed by integrating droplet-dispensed graphene oxide (GO) sensing elements and flexible electronics. The utilization of droplet-dispensing technology enables the fabrication multiple capacitive sensing elements rapidly while producing sensitive pressure sensors with excellent repeatability. The dispensed droplet volume (GO aqueous dispersion) ranged from around 33.5 to 65.4 pL with diameter ranging from 40 to 50 μm. The size (i.e., footprint and dielectric material thickness) of a sensing element can be controlled by the total GO dispersed per droplet. The fabrication process and preliminary characterization of these GO capacitive sensors are discussed in this paper. Thus far, we have shown that these sensors have a sensitivity of $\sim 10^{-3}$ kPa^{-1}, with the relative permittivity of the dispensed GO being $\sim$6 (measured at a frequency of 600 kHz). We have also demonstrated that the printed sensing elements can be used for human wrist pulse sensing. Hence the technology described in this paper could potentially be used in wearable electronics for healthcare applications.

INDEX TERMS Droplet dispensing, graphene oxide, tactile sensor, human pulse sensing, flexible sensors.

I. INTRODUCTION

Flexible electronics have become crucial because of their capability to monitor human health and physiological signals. However, the fabrication of high reliability, high sensitivity, and high repeatability sensors still relies on the microelectromechanical system (MEMS) fabrication process that requires sophisticated technology and MEMS knowledge, in addition to expensive machines. Apart from the complicated fabrication processes in MEMS, the materials used in MEMS fabrication mainly comprise silicon and other metals, such as copper and titanium, which intrinsically increase the hardness and decrease the flexibility of the sensors. 3D printing technology, the counterpart of MEMS fabrication, allows for quick prototyping and low-cost but effective sensor fabrication for flexible electronics. In the first part of the current literature review, MEMS fabrication and 3D printing technology are compared from different aspects to justify our use of 3D printers as our major tool. Pressure sensors involve many sensing mechanisms, including piezoresistive, piezoelectric, capacitive, and field-effect transistor (FET). These sensors are compared in the blow to identify the most suitable sensing mechanism for 3D printing of pressure sensors with improved sensitivity.

II. COMPARATION BETWEEN DIFFERENT SENSING MECHANISMS OF PRESSURE SENSOR

A pressure sensor is a device that can be used to perceive a pressure signal and then convert this signal to a type of electric signal that can be read by humans through certain mechanisms. Based on the working mechanisms, pressure sensors can be categorized as piezoresistive, piezoelectric,

TABLE 1. Comparison Different Type of Pressure Sensor From Physical Parameter [1]

	Capacitive	Piezoresistive	Piezoelectric	Optical
Miniaturization technique	• MEMS on Polymer/Si	• MEMS on Polymer/Si	• MEMS on Polymer/Si • Nanotechnology	• MEMS on Polymer
Force / Pressure sensitivity	• 0.028%/kPa (shf) – 14%/kPa • 50 mN (shf) – 190 mN (nf) • 7.7%/N – 67.2%/N	• 0.17%/kPa – 23%/kPa • 6.67%/N(nf) – 86.7%/N(shf)	• 430 mV/N	• /
Range of force (N)/Pressure (kPa)	• 0.5 – 140	• 1.8 – 163	• 2 – 275	• 3.9 – 4
No. of sensing element	• 2x2 – 13x10	• 1 – 2x2	• 1 – 12	• 1 – 3x3

optical fiber, and capacitive. These pressure sensors are commonly utilized in industries and research. In particular, the capacitive pressure sensor has many advantages over other pressure sensors. This sensor has low power consumption because no DC current flows through the sensor element. It uses current only when a pressure signal passes through the circuit, thereby measuring the capacitance. Passive sensors have an external reader, which provides a signal to the circuit; hence, a power supply is not needed. This feature is good for applications that require low power, such as e-skin sensors or remote monitoring.

A capacitive sensor is a mechanically simple device with a stable output, and it is compatible with complicated environments. Moreover, it has high tolerance for temporary over-pressure situations. The main merits of capacitive sensors are that they are independent of temperature and have good repeatability. However, capacitive sensors do not produce a linear output, and they may cause high hysteresis and increased sensitivity to vibration. However, they perform well in touch-mode devices because their diaphragm comes into contact with the insulating layer located on the lower electrode. One of the risks is that these sensors may damage sensitivity and increase hysteresis. Parasitic capacitance reduces the sensitivity and accuracy of capacitive sensors. A good circuit design is necessary for interface electronics with high output impedance to minimize the influence of parasitic capacitance. Placing numerous electronics close to the sensor improves the situation. This is one of the advantages of the MEMS technique. For hu-man-carry or e-skin devices, optical sensors perform poorly because they are uncomfortable and large. Meanwhile, piezoresistive sensors exhibit hysteresis and have high power consumption; therefore, they are unsuitable for e-skin device design. Although piezoelectric and capacitive sensors are highly sensitive and accurate, the former provides only dynamic sensing. Overall, capacitive sensors are a good choice for robotic e-skin device design.

After comparing the advantages, disadvantages, and different physical aspects (from the miniaturization technique to the number of sensing elements) of different pressure sensors, I conclude that capacitive pressure sensors are better than the others. They are highly sensitive and independent of temperature, as shown in Table 1. They also have many sensing elements in a single unit area. Our conclusion is that capacitive pressure sensors are more suitable for human e-skin device development compared with other sensors.

A. COMPARATION BETWEEN DIFFERENT FABRICATION METHODS

In related fabrication processes, MEMS pressure sensors can exhibit similar performance as 3D printing pressure sensors even though they are used in different scenarios. However, the reliability of MEMS devices and fabrication poses a major challenge. MEMS is developed based on semiconductor manufacturing technology, which integrates the technologies of lithography, corrosion, thin film, LIGA, silicon micromachining, non-silicon micromachining, and precision machining. Pressure sensors cannot avoid the original problems from semiconductor manufacturing technology. Such problems can be divided into six categories: mechanical fracture, stiction, wear, creep and fatigue, electric circuit, and contamination. For example, in the fabrication of graphene-resistive and optical-fiber pressure sensors, the holes, including the array of SiNx holes and the glass ferrule hole for the optical fiber, inevitably encounter the shock problem, which is related to mechanical interference dis-order, excessive loading, and drops. As indicated by the examples, 3D printing has several advantages over traditional MEMS fabrication in terms of fabrication processes, design difficulty, and required manpower. Notably, 3D printing pressure sensors focus on the principles and materials. In addition, MEMS fabrication needs a laboratory to implement the manufacturing process, whereas 3D printing has a compact layout.

However, the resolution of 3D printing is an issue that should be solved as soon as possible. Photolithography can reach a resolution of 1 micron, and laser direct write can reach 100 nm or even better. Current usable 3D printing is limited to 500 nm, which leads to the use of large-scale pressure sensors. Furthermore, 3D printing has high requirements for the materials' form (e.g., liquid-like), viscosity, particle size, temperature, and pressure. Considering that 3D printing is a multi-structure sensor manufacturing process, it cannot use directly laser sinter metal powder for printing or cooling and molding after melting polymer materials. As shown in the example above, the PVDF polymer and barium titanite are mixed and injected as dipoles under the substrate. At the same time, the entire process needs to be electrified, and

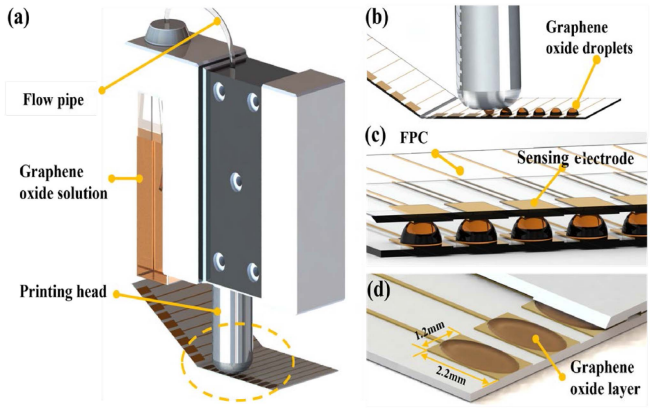

FIGURE 1. Fabrication of the sensing elements. (a) Printing setup, (b) Printing head and droplet, (c) and (d) Structure of the sensing elements.

electrostatic force is used to ensure a stable combination of the materials and substrate. As a result, the materials and resolution interact with and constrain each other.

On the other hand, tactile sensing is often considered as one of the most important possible technological extensfter comparing the advantages, disadvantages, and different physical aspectsions in robotic and automation systems since it provides another realm of information (i.e., touch) from physical interactions with the surrounding environment. Researchers have long been looking for more sensitive and flexible materials to be integrated into their robotic systems in order for robots to "feel" the physical world. Nowadays, Graphene oxide (GO) has been drawing much attention because of its unique mechanical, optical, electrical, and chemical properties [2], [3], [4], including high surface to volume ratio, easy and low cost to manufacture, ultra-thin and transparent. It has become a very attractive material for applications in flexible electronics and sensors, including applications to sense pressure [4], strain [5], temperature [6] and humidity [7]. Furthermore, GO can be chemically reduced to produce reduced-GO (r-GO) which could serve as a conductive electrode material. GO has also been reported to have a relatively high electric permittivity [8], [9], [10], [11], [12] and has been used as a dielectric material in pressure or tactile sensors [13], [14], with reported sensitivities ranging from 10-3 to 1kPa-1 [15], [16].

For the fabrication of GO based sensors, GO is often dispersed in water [16], [17] or mixed with other elastomers (e.g., PDMS) [18], [19]. Typically, the GO suspension is applied through spin coating or dropping. However, these techniques are complicated for fabricating multiple sensor arrays, especially if the patterning multiple GO layers is required.

In this paper, we presented a simple, low cost, and direct method of fabricating capacitive sensing elements using micro- dispensing of GO suspension. The GO layer is directly printed on top of sensing electrodes and its thickness (i.e., capacitance) can be easily controlled by droplet volume and number of printed layers. Sensing elements with different capacitances have been fabricated and characterized. Preliminary results on human pulse sensing are also reported. Based on our current results, we believe that the developed sensing elements can potentially be used in wearable sensors/electronics and healthcare applications.

TABLE 2. Printing Parameters of the Micro-Dispensing System in Printing the Go Suspension

Printing voltage	100V – 150V
Pulse width	20ms – 30ms
Droplet sizes	40μm – 50μm
Droplet volumes	33.5pL – 65.4pL

III. FABRICATION OF GO BASED SENSING ELEMENTS

A. FABRICATION PROCESS

A drop dispensing system (from Microdrop Technologies, Germany) was used to dispense GO suspension as shown in Fig. 1(a). The GO suspended water (with concentration of 2 mg/ml) (from Tanfeng, China [20]) was sonicated in a water bath for 15 minutes to homogenize the GO suspension. The printing voltage applied in our experiments varied from 100 V to 150 V with a pulse width of ∼20 to 30 ms. The ejected droplet sizes and volumes ranged from 40 to 50 μm and from 33.5 to 65.4 pL, respectively (Fig. 1(b)). The GO suspended droplets were printed layer by layer on copper electrodes to form GO-films on a flexible Printed Circuit Board (PCB). Before printing another layer, the printed layer was dried at 60 °C in order to avoid GO from being dissolved. Once the desired thickness of the GO-films is printed, another flexible PCB (thickness 0.2 mm) was put on top of the GO-films, resulting in a sandwiched structure of GO dielectric layer as shown in Fig. 1(c) and (d).

First, the GO suspended water (with a concentration of 2 mg/ml) (from Tanfeng, China) was sonicated in a water bath for 15 min to homogenize the GO suspension. Second, the printing voltage applied in the experiments varied from 100 V to 150 V with a pulse width of ∼20 ms to 30 ms, as shown in Table 2. The ejected droplet sizes and volumes ranged from 40 μm to 50 μm and from 33.5 pL to 65.4 pL, respectively, (Fig. 1(b)). The GO suspended droplets were printed layer by layer on copper electrodes to form GO-films on a flexible PCB, which was purchased from a commercial vendor. After printing each layer, the printed layer was dried at 60 °C to improve control in the GO-film and avoid the adjacent GO droplets merging together for having accumulated droplet size. Once the desired thickness of the GO-films is printed, another flexible PCB (0.2 mm thickness) was placed on top of the GO-printed PCB, resulting in a sandwiched structure of a GO dielectric layer, as shown in Fig. 1(c) and (d).

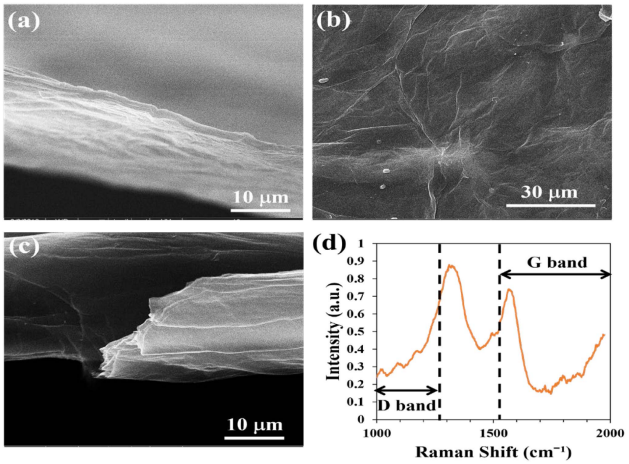

FIGURE 2. SEM pictures and Raman spectrum of a printed GO-film. (a) the surface and (b) Cross-section of GO on electrodes, (c) GO-film peeled off from electrode and (d) the Raman spectrum.

B. FABRICATED GO-FILMS

The Scanning Electron Microscopy (SEM) pictures and Raman spectrum of a printed GO-film are shown in Fig. 2. In Fig. 2(a) and (b), the surface and cross-section of the printed GO on the copper electrode are shown, respectively. Fig. 2(c) shows a peeled off GO-film from the electrode. It can be clearly seen that the GO-films contain numerous layers. The Raman spectrum also confirmed that the printed film retains the characteristics of GO as shown in Fig. 2(d). The D and G bands were measured around 1344 cm-1 and 1588 cm-1. The D band represents the presence of defect sites in the framework of GO due to the disorder induced by sp3 hybridization and the D band of GO is strong and broad because the graphene layers have high level of disorder; while the G band represents the in-plane bond-stretching motion of sp3 carbon atoms. The ID/IG ratio is 1.2.

IV. EXPERIMENTAL RESULTS

A. RELATIVE PERMITTIVITY OF THE PRINTED GO-FILMS

As shown in Fig. 1, the dimension of each sensing element in our current work is 2.2 mm × 1.2 mm. The thicknesses of the printed GO-films were measured by a surface profiler (DekTakXT from Bruker). Applying the equation below, the dielectric constant of the printed GO-film can be calculated.

$$C = \varepsilon_r \varepsilon_0 A \tag{1}$$

where C is the capacitance of the sensing element; ε_r is the relative permittivity (i.e., dielectric constant; relative permittivity ε_r of air is 1) of printed GO-film; ε_0 is the permittivity of free space (=8.854 × 10^{-12} Fm^{-1}); A is the area of the sensing element; and d is the distance between the top and bottom electrodes. In this experiment, GO-films were fabricated according to the procedure described in the last section. Five examples of the printed GO sensors and their measured parameters are shown in Table I. The calculated relative permittivity ε_r of the printed GO-films is ∼0.5 to 7.5 (measured at 600 kHz).

TABLE 3. Parameters of the Samples With Go-Films

Sensor	A	B	C	D	E
GO concentration (mg/ml)	2	2	2	2	5
Measured GO Layer Thickness (μm)	0.7	2.5	4.1	5.0	7.4
Measured Initial Capacitance (pF)	19.20	18.73	35.12	21.20	23.46
Max Capacitance at 20kPa (pF) *measured at 600kHz*	21.23	20.10	36.67	23.90	26.75
Calculated Relative Permittivity	0.57	2.00	6.16	4.53	7.43
Sensitivity(kPa^{-1})	0.0027	0.0020	0.0006	0.0002	0.0036

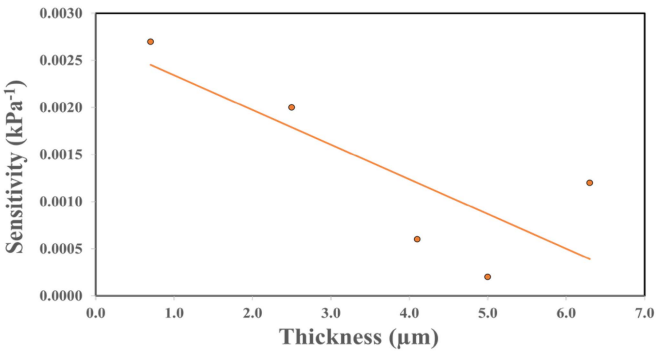

FIGURE 3. Variation of sensitivity with vs thickness of the sensing elements.

B. SENSITIVITY

In order to fabricate a useful pressure sensor, high responsivity and sensitivity are of prime importance. Since the sensing elements are capacitive type, the relationship between capacitance changes and applied pressure is first determined. The sensors, listed in Table 3, were tested under an applied pressure ranging from 0 to 20 kPa, which often uses in human pulse detection [21]. The sensitivity S is calculated using the following equation:

$$S = \frac{1}{C_0}\frac{\Delta C}{\Delta P} \tag{2}$$

where C_0 is the initial capacitance; ΔC is the change in capacitance; and ΔP is the change in pressure. The sensitivity changes clearly along with the thickness of the printed GO layer. As shown in Fig. 3, the sensitivity decreases linearly from 0.0027 kPa^{-1} to 0.0002 kPa^{-1} as the GO layer thickness increases.

Moreover, as shown in Fig. 4, if the GO concentration is further increased to 5 mg/ml (i.e., sensor E), the corresponding sensitivity will be increased to 0.0036 kPa-1, which is more than 10 times of that of 2 mg/ml with similar thickness. The

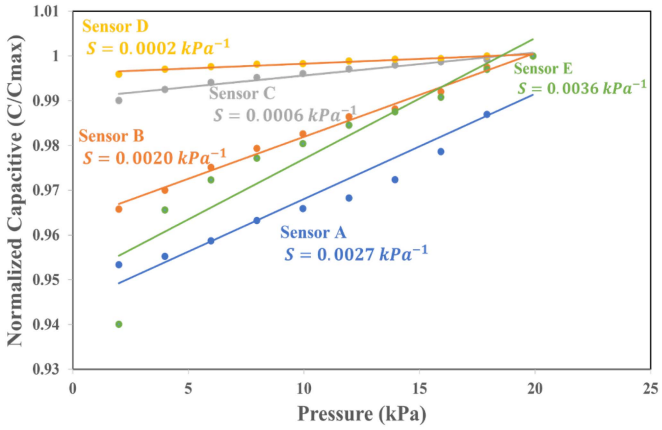

FIGURE 4. Capacitance change vs pressure applied on the sensing elements.

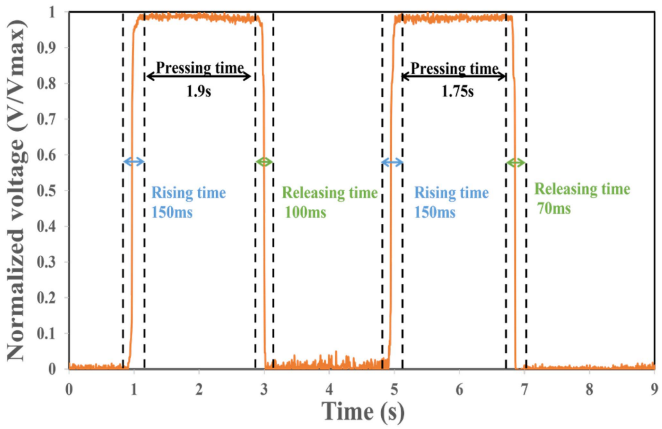

FIGURE 5. Instantaneous response of a sensing element.

main reason may be due to the increase in GO concentration per volume printed. Thus, when the GO suspension is dried, more GO will be closely packed on top of the electrode. In other words, the GO/air ratio will be increased, and thus, the ε_r will be increased, consequently improving the sensitivity.

C. INSTANTANEOUS RESPONSE

The instantaneous response is an important factor for designing a sensing element. In this experiment, an instantaneous pressure of 20 kPa was applied to sensor E for a short duration (2 seconds) and the result is shown in Fig. 5. The response time is ∼100 to 150 ms, which is fast enough to capture human pulse, which is usually lower than 2 Hz [21].

D. HUMAN PULSE SENSING

Arterial pulses, which are generated by heart-pumping of blood, reflect the holistic health status of human. In Traditional Chinese Medicine (TCM), there are 28 basic combinations of well-known pulse patterns [22]. The detection of human pulses is one of the important applications in wearable electronics and healthcare. In this study, we preliminary tested the detection of human pulses using the

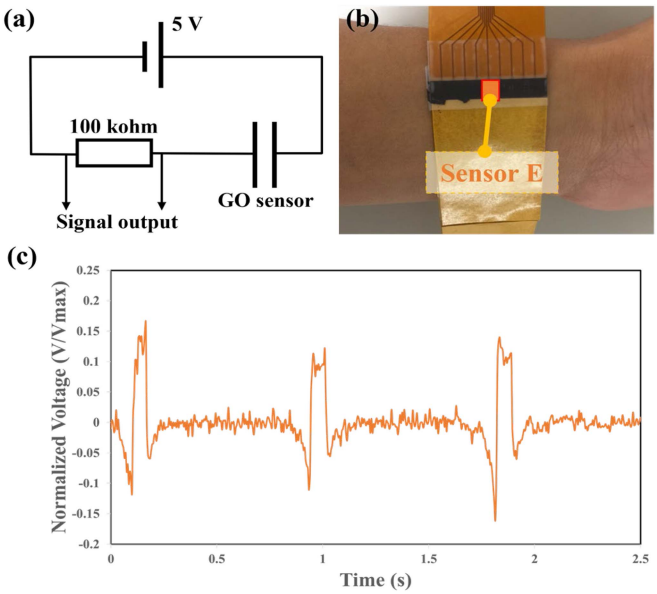

FIGURE 6. Human pulse detection using sensor E. (a) Circuit for data acquisition, (b) Sensor placement, and (c) the recorded signal.

fabricated GO sensing elements. The sensor E's circuit, with a sampling rate of 200 MHz, used for signal detection is shown in Fig. 6(a). It was placed on a subject's wrist for pulse detection as shown in Fig. 6(b). The recorded and normalized signal is shown in Fig. 6(c). The collected data shows a clear main peak and several sub-peaks. The recorded pulse rate was ∼72 beats/min. Currently, the sensors reported here are not as responsive to pressure input as the commercial capacitive sensors reported in [21] 0.00031 kPa^{-1}. One of the possible reasons is that the flexible PCB used is too thick (i.e., 0.2 mm) and stiff, which will reduce mechanical responsivity of the sensor and suppresses the weak reflected-pulse signals (i.e., the higher frequency small peaks in the pulse response signals in Fig. 6(c)). Another way to improve it is to further increase the GO concentration in the suspension.

E. MULTIPLE ELEMENT SENSING

In the last section, the pulse recording was done by a single sensor. Indeed, much more information (i.e., spatial pressure distribution) can be captured if a sensing array can be built. For demonstration purpose, a sensing array containing 9 elements from C1 to C9 was fabricated using GO-films as the dielectric as shown in Fig. 7(b). The structure of the sensing array is shown in Fig. 7(a). A constant and static pressure (i.e., 20 kPa) is applied near C8, C9, C5 and C6. The recorded capacitance values and normalized 3D position map of the normalized change in capacitances are shown in Fig. 7(c). The map is plotted using cubic interpolation function. The values printed on the map are the capacitances of the sensing elements when the pressure is applied. With this technique, the spatial pressure distribution of a human pulse can be easily resolved.

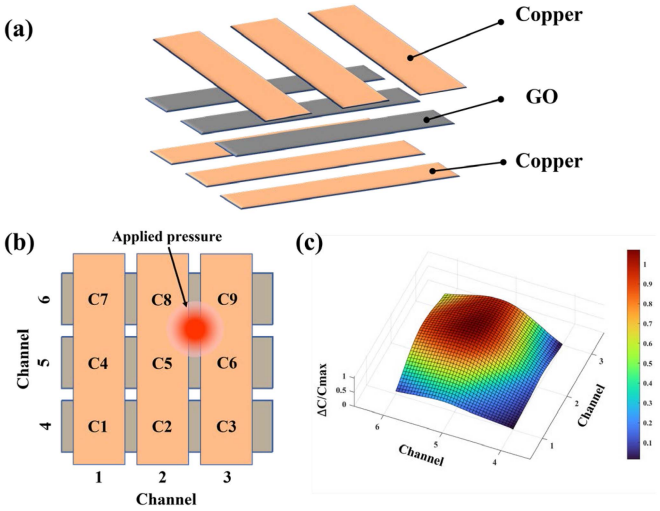

FIGURE 7. An example of a fabricated GO-based sensing array. (a) the structure of the sensing array, (b) Sensing array and (c) Color-interpolated position map.

V. GO SENSOR FABRICATION USING SPUTTERING

In summary, our preliminary results on fabricating a novel flexible pressure sensor array by micro-dispensing of GO suspension were reported. The printed sensors were characterized and demonstrated to be capable of acquiring human pulse pressures. More detailed studies are underway (i.e., the effect of different printing parameters on electrical and mechanical properties of the printed sensing elements) to better control the performance of each sensing element. Combined with the development of machine learning algorithms on human wrist pulse patterns, a wearable electronic device can be realized to collect and monitor personalized health data for healthcare applications in the future.

A. SENSOR FABRICATION – CONDUCTIVE LAYER

The preliminary results on the fabrication of a flexible capacitive sensing array using GO as the sensing material reported about a fabrication process of producing dielectric and conductive layers by using a direct material deposition method, which would enable the fabrication of final sensing devices by means of vertically assembled structures. Thus far, the best sensitivity of our fabricated sensor was 0.00031 kpa^{-1}, and the transient response time is ~40 ms. The abilities of the sensors in showing static spatial pressure distribution and capturing dynamic temporal human pulse were demonstrated, which showed the potential application of these novel flexible sensing array in wearable electronics.

The potential of using GO as a dielectric layer of capacitive pressure sensors is demonstrated above, which mainly used a micro-dispensing method to achieve a precise, low-cost, and effective sensor fabrication process. However, to increase the flexibility of the pressure sensing array, the electrodes on the PET (polyethylene terephthalate) substrate should be replaced by soft materials such as PDMS (polydimethylsiloxane). Based on previous works of fabricating GO-films,

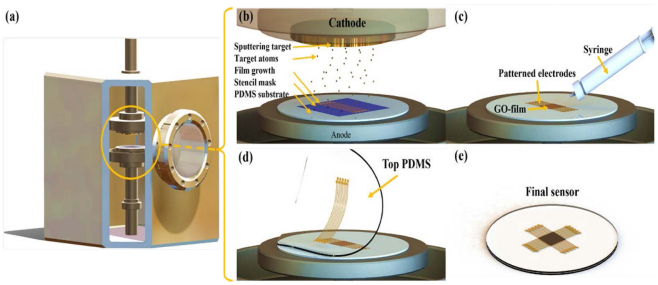

FIGURE 8. Fabrication process: (a) Overview of inside the sputtering machine. (b) Using a stencil mask to transfer patterns onto PDMS surface. (c) Depositing GO-film on top of electrodes. (d) Stacking another PDMS to form a sandwiched structure. (e) Fabricated flexible sensing device.

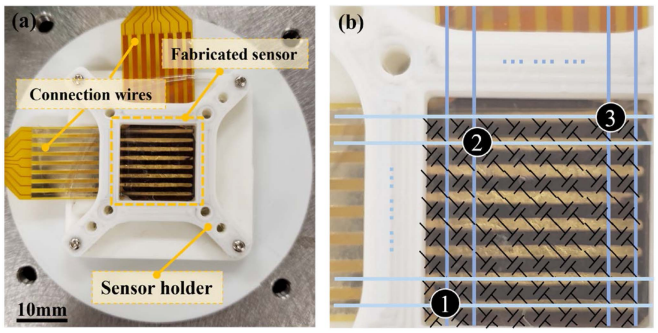

FIGURE 9. Overview of the assembled sensor for sensor characterizations: (a) Two pieces of flexible PCBs mounted to the fabricated sensor by holder. (b) 3 locations of capacitive sensing elements.

deposition of designated materials on substrates was feasible, especially in multi-layer structures. Hence, a similar mechanism was adapted in our current work to fabricate electrodes and GO-based sensing elements.

B. PROPOSED FABRICATION PROCESS AND SENSOR CHARACTERISTICS

Reduced graphene oxide (rGO) and carbon nanotube (CNT) were first tested by screen printing methods to form a conductive layer of capacitive tactile sensors which contain electrode patterns transferred from designed stencil mask. However, these materials were found difficult to attach on the surface of PDMS, leading to disconnected or partially formed electrodes with tremendously high resistance, i.e., up to 100 kOhm. In fact, sputtering gold target onto the surface of PDMS (with a thickness of 0.5 mm) was applied to obtain electrodes with conductivity of 166.67–714.29 mS/m (the fabrication process is shown in Fig. 8). In this chapter, the GO-films were deposited on top of the electrodes by a syringe, instead of a micro-dispensing system reported from previous chapter. A sandwiched structure was then formed by stacking another PDMS (with a thickness of 0.5 mm) with same pattern of electrodes. The final device was mounted to connect an external circuit, as shown in Fig. 9, for sensor characterization.

Each sensing element was applied with various static pressure to measure its capacitance changes by using the setup of

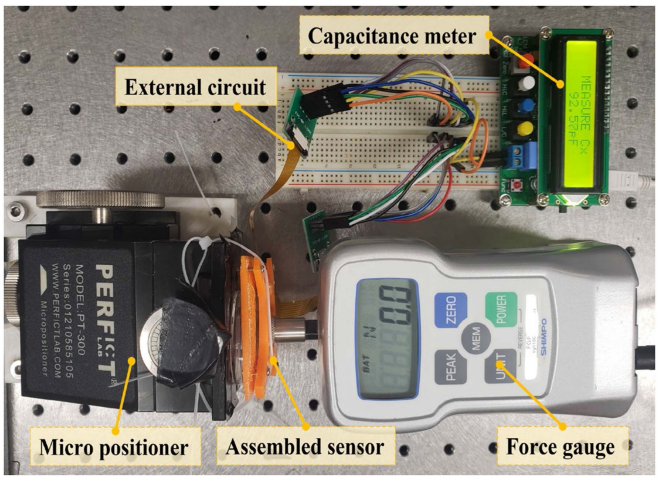

FIGURE 10. Experimental setup for measuring sensor capacitance changes.

TABLE 4. Sensor Parameters for the Sensing Elements

Sensing element	C1	C2	C3	C4	C5
Initial Capacitance (pF)	238.8	576.92	95.508	80.6	120.58
Maximum Capacitance at 5MPa (pF)	297.84	636.8	102.02	86.27	145.64
Sensitivity at low pressure range (kPa^{-1})	0.00020	0.00003	0.00031	0.00027	0.00008
Sensitivity at high pressure range (kPa^{-1})	0.00020	0.00020	0.00002	0.00002	0.00008

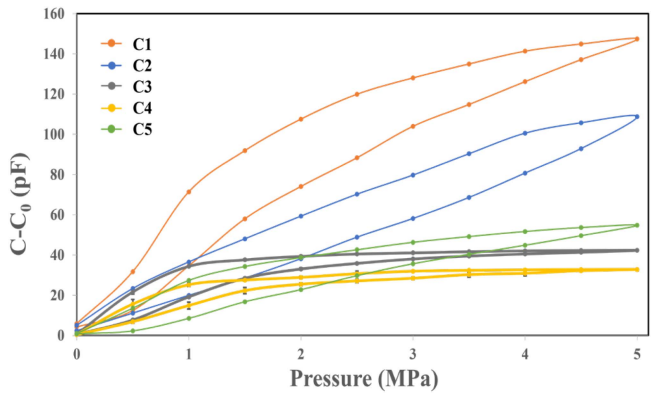

FIGURE 11. Capacitance changes under applied pressure.

Fig. 10 to characterize the fabricated sensor. The characterized sensor parameters are shown in Table 4. The difference of sensitivity among each element was due to the process of GO-film deposition. The capacitance changes under pressure of C1-C5 are shown in Fig. 11.

In comparison with previous research on GO-film fabrication, changing the conductive layer from electrodes on PET to PDMS showed an inconsiderable effect on sensor sensitivity. After characterizing each element of the sensing array, the response time was measured by applying an instant force

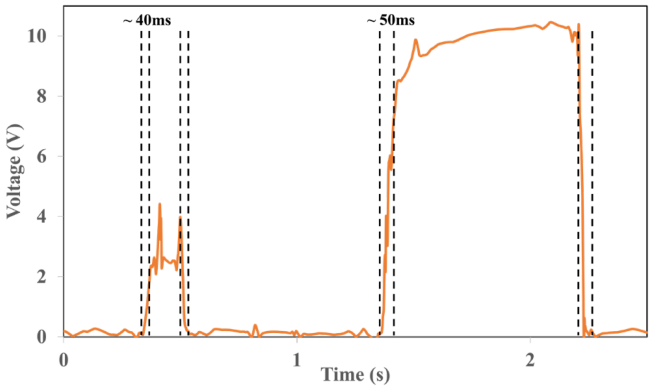

FIGURE 12. Response characteristic of a fabricated sensing element.

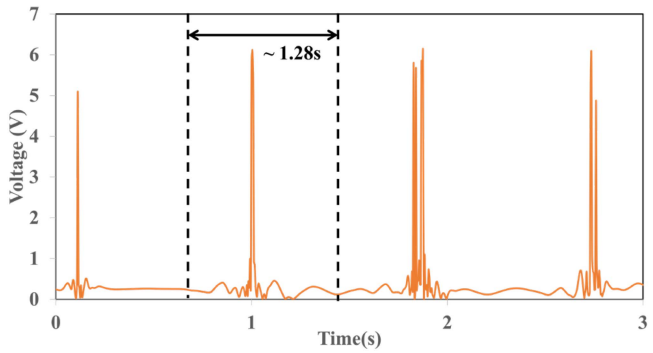

FIGURE 13. Human pulse capturing using a single sensing element.

(1 and 5 N), as shown in Fig. 12, and the corresponding response was ~40–50 ms. Given that the ability of using the sensors to capture human pulse pressure is of prime importance to our application, the device was put on a wrist of a person who had a heart rate of 74 bpm to record human pulse. In Fig. 13, the measured rate of this subject was 72 bmp.

The advantages of direct deposition of multiple materials using shadow masks could easily achieve an efficient nanofabrication process because the thickness of the overall device could be easily controlled by the deposited layers and PDMS substrate (e.g., fabricating ultra-thin tactile or pulse-pressure sensors for the application of wearable electronics).

The idea of fabricating sensing electrodes by sputtering on stencil masks was proven to accomplish the main component for a flexible sensor. However, the design was particularly rough to achieve our ultimate application. Accordingly, two different stencil masks were made by commercial vendors utilizing laser drilling to fabricate high precision masks. The aforementioned fabrication process was repeated but with a different mask. In Fig. 14, the micro-dispensing process was performed on a non-plasma (Fig. 14(a)) and a plasma surface (Fig. 14(b)). A hydrophobic surface would lead to a partial electrode coverage because the top layer was later placed on top of the GO-films. Hence, a hydrophilic surface would be ideal to avoid short circuit.

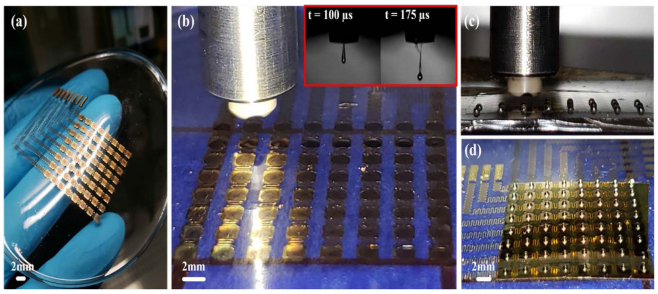

FIGURE 14. Micro-dispensing of the droplets of the graphene solutions on au-sputtered PDMS. (a) Printed substrate, (b) Micro-dispensing after plasma treatment, and (c) Droplet printing process, and (d) Printed droplet array.

VI. CONCLUSION

In this paper, we presented our preliminary results on fabricating a novel flexible pressure sensor array by micro- dispensing of GO suspension. The printed sensors were characterized and have been demonstrated to be capable of acquiring human pulse pressures. More detailed and intensive studies are underway to study the effect of different printing parameters on electrical and mechanical properties of the printed sensing elements in order better control the performance of each sensing elements. Together with the development of this technology and existing classification algorithms on human wrist pulses, a wearable electronic device can be realized to collect and monitor personalized health data for healthcare applications in the future.

REFERENCES

[1] Y. Al-Handarish et al., "A survey of tactile-sensing systems and their applications in biomedical engineering," *Adv. Mater. Sci. Eng.*, vol. 2020, 2020, Art. no. 4047937.

[2] K. Novoselov, "Electric field effect in atomically thin carbon films," *Science*, vol. 306, no. 5696, pp. 666–669, 2004.

[3] Y. Zhu et al., "Graphene and graphene oxide: Synthesis, properties, and applications," *Adv. Mater.*, vol. 22, no. 35, pp. 3906–3924, Sep. 2010.

[4] A. Balandin et al., "Superior thermal conductivity of single-layer graphene," *Nano Lett.*, vol. 8, no. 3, pp. 902–907, 2008.

[5] Y. Luo, Q. Xiao, and B. Li, "A stretchable pressure-sensitive array based on polymer matrix," *Sensors*, vol. 17, no. 7, 2017, Art. no. 1571.

[6] S. Kundu, R. Sriramdas, K. R. Amin, A. Bid, R. Pratap, and N. Ravishankar, "Crumpled sheets of reduced graphene oxide as a highly sensitive, robust and versatile strain/pressure sensor," *Nanoscale*, vol. 9, no. 27, pp. 9581–9588, 2017.

[7] R. Kazemzadeh and W. S. Kim, "Flexible temperature sensor with laser scribed Graphene oxide," in *Proc. 14th IEEE Int. Conf. Nanotechnol.*, 2014, pp. 420–423.

[8] X. Huang et al., "Graphene oxide dielectric permittivity at GHz and its applications for wireless humidity sensing," *Sci. Rep.*, vol. 8, no. 1, pp. 1–7, 2018.

[9] J. Liu, D. Galpaya, M. Notarianni, C. Yan, and N. Motta, "Graphene-based thin film supercapacitor with graphene oxide as dielectric spacer," *Appl. Phys. Lett.*, vol. 103, no. 6, 2013, Art. no. 063108.

[10] D. Sinar and G. Knopf, "Printed graphene interdigitated capacitive sensors on flexible polyimide substrates," in *Proc. 14th IEEE Int. Conf. Nanotechnol.*, 2014, pp. 538–542.

[11] R. Kazemzadeh, K. Andersen, L. Motha, and W. S. Kim, "Highly sensitive pressure sensor array with photothermally reduced graphene oxide," *IEEE Electron. Device Lett.*, vol. 36, no. 2, pp. 180–182, Feb. 2015.

[12] M. Kang, J. Kim, B. Jang, Y. Chae, J. Kim, and J. Ahn, "Graphene-based three-dimensional capacitive touch sensor for wearable electronics," *ACS Nano*, vol. 11, no. 8, pp. 7950–7957, 2017.

[13] G. Khurana, N. Kumar, S. Kooriyattil, and R. Katiyar, "Structural, magnetic, and dielectric properties of graphene oxide/$Zn_xFe_{1-x}Fe_2O_4$ composites," *J. Appl. Phys.*, vol. 117, no. 17, 2015, Art. no. 17E106.

[14] P. Liu, Z. Yao, and J. Zhou, "Mechanical, thermal and dielectric properties of graphene oxide/polyimide resin composite," *High Perform. Polymers*, vol. 28, no. 9, pp. 1033–1042, 2016.

[15] K. Kumar, S. Pittala, S. Sanyadanam, and P. Paik, "A new single/few-layered graphene oxide with a high dielectric constant of 106: Contribution of defects and functional groups," *RSC Adv.*, vol. 5, no. 19, pp. 14768–14779, 2015.

[16] S. Wan et al., "Graphene oxide as high-performance dielectric materials for capacitive pressure sensors," *Carbon*, vol. 114, pp. 209–216, 2017.

[17] H. Tian et al., "A graphene-based resistive pressure sensor with record-high sensitivity in a wide pressure range," *Sci. Rep.*, vol. 5, no. 1, pp. 1–6, 2015.

[18] J. Paredes, S. Villar-Rodil, A. Martínez-Alonso, and J. Tascón, "Graphene oxide dispersions in organic solvents," *Langmuir*, vol. 24, no. 19, pp. 10560–10564, 2008.

[19] D. Dreyer, S. Park, C. Bielawski, and R. Ruoff, "The chemistry of graphene oxide," *Chem. Soc. Rev.*, vol. 39, no. 1, pp. 228–240, 2010.

[20] H. Qiao et al., "Preparation of graphene oxide/bio-based elastomer nanocomposites through polymer design and interface tailoring," *Polym. Chem.*, vol. 6, no. 34, pp. 6140–6151, 2015.

[21] J. Tang et al., "Study on a novel composite coating based on PDMS doped with modified graphene oxide," *J. Coatings Technol. Res.*, vol. 15, no. 2, pp. 375–383, 2018.

[22] K. Kong et al., "A pulse-sensing robotic hand for tactile arterial palpation," in *Proc. IEEE Int. Conf. Cyber Technol. Automat. Control Intell. Syst.*, 2016, pp. 141–145.

[23] Z. Xie, "Selected terms in traditional Chinese medicine and their interpretations XVI," *Chin. J. Integr. Med.*, vol. 22, no. 140, pp. 223–226, 2001.